

Charge exchange produced emission of carbon in the extreme ultraviolet spectral region

This content has been downloaded from IOPscience. Please scroll down to see the full text.

View [the table of contents for this issue](#), or go to the [journal homepage](#) for more

Download details:

IP Address: 198.125.233.17

This content was downloaded on 09/07/2015 at 20:11

Please note that [terms and conditions apply](#).

Charge exchange produced emission of carbon in the extreme ultraviolet spectral region

J K Lepson¹, P Beiersdorfer², M Bitter³, A L Roquemore³, K Hill³
and R Kaita³

¹ Space Sciences Laboratory, University of California, Berkeley, CA 94720 USA

² Physics Division, Lawrence Livermore National Laboratory, Livermore, CA 94550 USA

³ Princeton Plasma Physics Laboratory, Princeton, NJ 08543 USA USA

E-mail: lepson@ssl.berkeley.edu

Abstract.

We used a time-resolving high-resolution grating spectrometer to study extreme ultraviolet emission from plasmas in the National Spherical Tokamak Experiment (NSTX). The NSTX spectral range from 150-250 Å is typically dominated by emission from M-shell iron lines, L-shell transitions of oxygen, or K-shell lines of lithium. However, we also observed several intense emission lines, which we now attribute to transitions in C V and C VI. Collisional-radiative modeling shows that electron-impact excitation is far too weak to account for the features we observed. Instead, these lines appear to be produced by charge exchange with neutral hydrogen.

1. Introduction

Charge exchange occurs when an ion takes an electron from a neutral species or from an ion with lesser charge, thereby reducing its own charge while increasing the charge of the donor species. In recent years, it has been identified as an important process in astrophysics, where it contributes to the soft x-ray background. Charge exchange occurs extensively in the solar system, e.g., in the interaction of neutral atoms of cometary comae and planetary atmospheres with the highly charged solar wind [1, 2, 3], and may also be a significant source of soft x rays in such objects as supernova remnants and starburst galaxies [4, 5]. Charge exchange is also of interest as a diagnostic tool in tokamaks, especially for determining ion temperature and impurity profiles using an energetic neutral beam to enable charge exchange deep within the plasma [6, 7, 8].

Spectral observations of astrophysical charge exchange phenomena have mainly focused on the x-ray emission of K-shell ions. Identifying lines produced by charge exchange in the extreme ultraviolet (EUV) region may aid in ascertaining charge exchange phenomena in cooler plasmas. Both the *Chandra* and *XMM-Newton* x-ray observatories are sensitive to EUV emission from cosmic sources, while the *Hinode* satellite and the *Solar Dynamics Observatory* observe this spectral band in the sun. Thus, it may be possible to use these currently operating observatories to search for lines indicative of charge exchange.

In recent years we have made measurements of the EUV emission spectra generated by the NSTX spherical torus [9, 10, 11]. The focus of these measurements has been to study the iron L-shell and iron M-shell emission and to calibrate density-sensitive line ratios [11, 12].



While studying the M-shell iron emission in the 170–250 Å region, we observed unexpected enhancements of some of the lines in this region, which initially appeared to be iron lines. Upon additional studies, we attributed the lines to transitions in carbon C V and C VI [15]. In the following, we present spectral data from NSTX discharges that have no noticeable iron emission. This confirms that the lines in question are not from iron. A comparison of the observed carbon emission with spectral calculations rules out that the lines are produced by electron-impact excitation. This leaves charge exchange as the production mechanism.

2. Experiment

We obtained spectra on NSTX using the Long-Wavelength EUV Spectrometer (LoWEUS; [11]) instrument. LoWEUS is a flat-field grating spectrometer with variable line spacing and a mean 1200 ℓ/mm . The spectral resolution is ~ 0.3 Å, resulting in a resolving power $\lambda/\Delta\lambda \sim 500\text{--}800$ in the 150–250 Å region we examined ([16]). LoWEUS is capable of a time resolution of ~ 5 ms, but was operated in time-integrated mode during the shot we present here. We operate a similar instrument on the Alcator tokamak [17, 18].

Figure 1 shows a spectrum from NSTX shot 140324. The strongest line in the spectrum is the Li III $2p \rightarrow 1s$ Lyman- α transition at 133 Å. The $2p \rightarrow 1s$ emission from heliumlike Li II can be seen just below 200 Å. The other strong lines are all from carbon, i.e., they are K-shell transitions from C V and C VI. Although these lines occur near 41 and 33 Å, respectively, they appear here in higher order diffraction. The fact that these carbon lines are seen proves the abundance of carbon in the plasma.

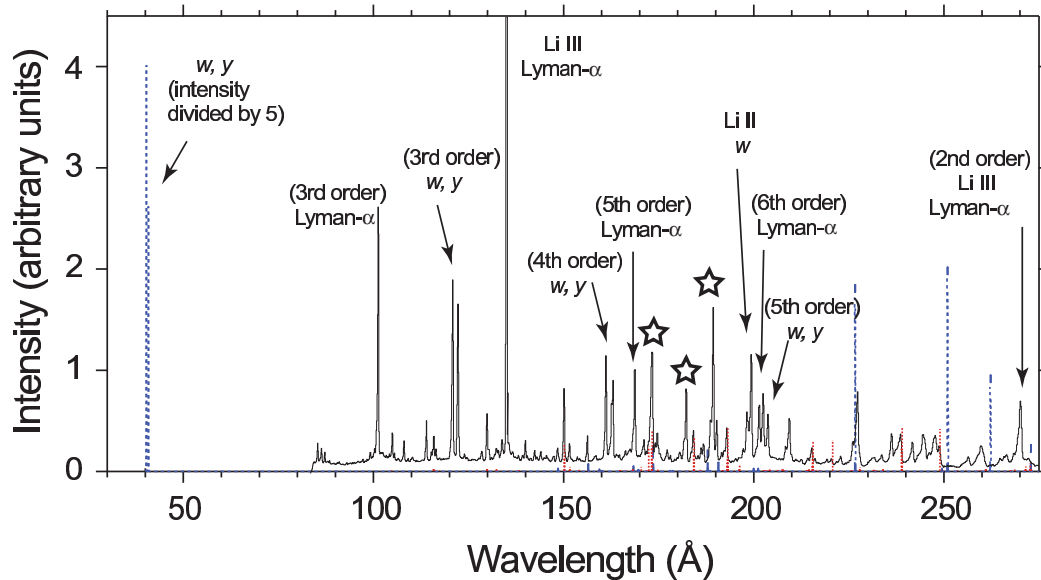


Figure 1. NSTX Shot 140324 (solid line) overlaid with FAC calculations of carbon emission due to collisional excitation (blue dashed lines) and oxygen emission from the CHIANTI database (red dotted lines). Intensities of carbon IV lines w and y in first order have been decreased by a factor of 5 to fit on the figure. Lines not identified to element are carbon; strong new carbon lines are marked with stars.

It is interesting to note that the the K-shell spectrum of heliumlike C V is comprised of two lines, commonly known as w and y , which emanate from the upper levels $1s2p^1P_1$ and $1s2p^3P_1$,

Table 1. Candidate carbon lines in the 170– 250 Å region.

Ion	Wavelength (Å)	Lower Level	Upper Level
C V	173.281	$1s2s\ ^3P_1$	$1s4p\ ^3P_1$
C VI	182.088	$2p\ ^2P_{1/2}$	$3d\ ^2D_{3/2}$
C VI	182.097	$2p\ ^2P_{1/2}$	$3d\ ^2D_{3/2}$
C VI	182.132	$2p\ ^2P_{1/2}$	$3d\ ^2D_{1/2}$
C VI	182.144	$2p\ ^2P_{1/2}$	$3d\ ^2D_{1/2}$
C VI	182.230	$2p\ ^2P_{3/2}$	$3d\ ^2D_{5/2}$
C VI	182.246	$2p\ ^2P_{3/2}$	$3d\ ^2D_{3/2}$
C VI	182.290	$2p\ ^2P_{3/2}$	$3d\ ^2D_{1/2}$
C V	189.255	$1s2p\ ^3P_1$	$1s4s\ ^3S_1$
C V	189.260	$1s2p\ ^3P_0$	$1s4s\ ^3S_1$
C V	189.304	$1s2p\ ^3P_2$	$1s4s\ ^3S_1$
C V	227.190	$1s2s\ ^3S_1$	$1s3p\ ^3P_2$
C V	227.202	$1s2s\ ^3S_1$	$1s3p\ ^3P_0$
C V	227.203	$1s2s\ ^3S_1$	$1s3p\ ^3P_1$
C V	248.660	$1s2p\ ^3P_1$	$1s3d\ ^3D_2$
C V	248.660	$1s2p\ ^3P_1$	$1s3d\ ^3D_1$
C V	248.672	$1s2p\ ^3P_0$	$1s3d\ ^3D_1$
C V	248.740	$1s2p\ ^3P_2$	$1s3d\ ^3D_3$
C V	248.748	$1s2p\ ^3P_2$	$1s3d\ ^3D_1$
C V	248.748	$1s2p\ ^3P_2$	$1s3d\ ^3D_2$

respectively.

Several weaker lines can also be seen. We have not yet identified all lines, but many of the weaker lines can be attributed to oxygen. The positions and relative intensities of the oxygen lines in this wavelength band are given by the CHIANTI spectral model [19, 20], as indicated by the red dotted lines in Fig. 1.

The spectrum in Fig. 1 also shows three relatively strong features marked with an asterisk. These are the features we have recently attributed to the carbon lines listed in Table 1.

3. Comparison with Theoretical Spectra

Calculations of the carbon line emission from collisional excitation were performed using the Flexible Atomic Code [21]. The line emission was calculated for the temperature of maximum abundance for C V (31 eV) and C VI (87 eV), using the electron density $n_e = 5 \times 10^{13} \text{cm}^{-3}$ measured by Thomson scattering. Calculations with higher and lower densities were also performed, but an effect of the density on the relative line emission could not be seen unless the density was varied by several orders of magnitude.

The results from our calculations for C V are shown in Fig. 1 as blue dashed traces. Here, we also show the w and y lines in 1st order. These lines appear in the spectrum only in 3rd and higher orders. We have normalized the intensity of the calculated emission in 1st order to the observed emission in 3rd order with the help of a measurement of the grating efficiency for measuring the w line in different orders made at the EBIT-I machine [22]. Because the first-order w and y lines are much stronger than the higher orders we observed, the NSTX spectrum and the calculated lines in the region we observed have been expanded vertically by a factor of 5 in order to better see the lines.

Our calculations predict several C V lines that fall into the observed spectral range. The largest predicted lines are near 228 and 251 Å, and they are stronger than any of the observed features. This may mean that our normalization to the 3rd order K-shell lines of C V is off by

several factors, thus resulting in an overprediction of these intensity of these lines. Despite this overprediction, the predicted intensity of the lines in question near 173, 182, and 189 Å is far too weak to account for the intensity of these carbon lines.

Figure 2 shows an expanded view of the spectral region near the three carbon features. The figure clearly demonstrates that the strengths predicted in our FAC model are vanishingly small. This rules out electron-impact excitation as the process forming these lines.

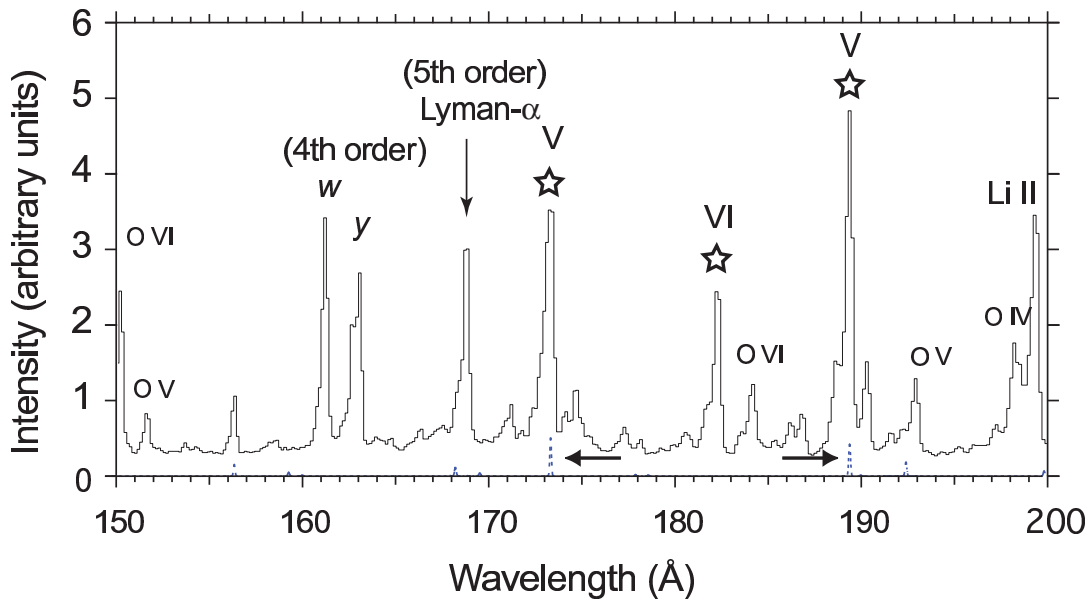


Figure 2. Inset of NSTX Shot 140324 showing comparison between calculated emission strengths via collisional excitation (blue dashed lines) vs. measured (solid line). Lines not identified to element are carbon; strong new carbon lines are marked with stars.

The strength of the new C V and C VI lines in our spectrum is indicative of non-equilibrium plasma processes, in particular, of charge exchange between highly charged carbon with neutral hydrogen. Charge exchange populates the $n = 3, 4$ levels in carbon ions, and our two strongest lines, at 173.19 and 189.40 Å are both $4 \rightarrow 2$ transitions, while the feature at 182.23 Å is a blend of $3 \rightarrow 2$ transitions. We are now undertaking calculations of the spectral emission due to charge exchange between hydrogen and bare and hydrogenlike carbon utilizing the Charge Exchange Spectral Synthesizer, CHESS [8]. CHESS predicts spectral emission patterns that match the observations well. These calculations are ongoing and will be presented in future work.

Acknowledgments

This work was performed by Lawrence Livermore National Laboratory and Princeton Plasma Physics Laboratory under the auspices of the U. S. Department of Energy under Contracts DEAC52-07NA27344 and DE-AC02-09CH11466 and supported by the U.S. Department of Energy, Office of Science, Office of Fusion Energy Sciences.

References

- [1] Cravens T E 2002, *Science*, **296**, 1042
- [2] Beiersdorfer P, Boyce K R, Brown G V, Chen H, Kahn S M, Kelley R L, May M, Olson R E, Porter F S, Stahle C K and Tillotson W A 2003, *Science*, **300**, 1558.

- [3] Wargelin B J, Beiersdorfer P, Neill P A, Olson R E and Scofield J H 2005, *Astrophys.J.Suppl.*, **634**, 637.
- [4] Katsuda S, Tsunemi H, Mori K, Uchida H, Kosugi H, Kimura M, Nakajima H, Takakura S, Petre R, Hewitt J W and Yamaguchi H 2011, *Astrophys.J.*, **730**, 24.
- [5] Wang Q D and Liu J 2012, *Astron.Nachrichten*, **333**, 373.
- [6] Källne E, Källne J, Dalgarno A, Marmar E S, Rice J E and Pradhan, A K 1984, *Phys.Rev.Lett.*, **52**, 2245
- [7] Rice J E, Marmar E S, Terry J L, Källne E and Källne J 1986, *Phys.Rev.Lett.*, **56**, 50.
- [8] Beiersdorfer P, Bitter M, Marion M and Olson R E 2005, *PhysRevA*, **72**, 032725.
- [9] Beiersdorfer P, Bitter M, Roquemore L, Lepson J K and Gu M F 2006, *Rev.Sci.Instrum.*, **77**, 10F306.
- [10] Beiersdorfer P, Lepson J K, Bitter M, Hill K W and Roquemore L 2008, *Rev.Sci.Instrum.*, **79**, 10E313.
- [11] Lepson J K, Beiersdorfer P, Clementson J, Gu M F, Bitter M, Roquemore L, Kaita R, Cox P G and Safronova A S 2010, *J.Phys.B*, **43**, 142010.
- [12] Lepson J K, Beiersdorfer P, Gu M F, Desai P, Bitter M, Roquemore L and Reinke M L 2012, *AIPConf.Proc.* **1438**, 136.
- [13] Beiersdorfer P, Crespo López-Urrutia J R, Springer P, Utter S B and Wong K L 1999, *Rev.Sci.Instrum.*, **70**, 276.
- [14] Graf A, Brockington S, Horton R, Howard S, Hwang D, Beiersdorfer P, Clementson J, Hill D, May M, Mclean H, Wood R, Bitter M, Terry J, Rowan W L, Lepson J K and Delgado-Aparicio L 2008, *Can.J.Phys.*, **86**, 307.
- [15] Lepson J K, Beiersdorfer P, Bitter M, Roquemore A L, Kaita R 2013, *PhysicaScripta*, **156**, 014075.
- [16] Lepson J K, Beiersdorfer P, Bitter M, Roquemore L, Hill K W, Kaita R, Skinner C H and Zimmer G 2012, *Rev.Sci.Instrum.*, **83**, 10D520.
- [17] Reinke M L, Beiersdorfer P, Howard N T, Magee E W, Podpaly Y, Rice J E and Terry J L 2010, *Rev.Sci.Instrum.*, **81**, 10D736.
- [18] Beiersdorfer P, Brown G V, Kamp J B, Magee E W, Lepson J K, Podpaly Y and Reinke M L 2011, *Can.J.Phys.*, **89**, 653.
- [19] Dere K P, Landi E, Mason H E, Monsignori Fossi B C and Young P R 1997, *Astron.Astrophys.Suppl.*, **125**, 149.
- [20] Landi E, Del Zanna G, Young P R, Dere K P and Mason H E 2012, *Astrophys.J.*, **S744**, 99.
- [21] Gu M F 2008, *Can.J.Phys.*, **86**, 675.
- [22] Brown G V, Beiersdorfer P, Clementson J, Dunn J, Kelley, R L, Kilbourne C A, Leutenegger M, Magee E W, Park J, Porter F S, Schneider M and Träbert E 2010, *Space Telescopes and Instrumentation 2010: Ultraviolet to Gamma Ray*. Ed. by Arnaud, Monique; Murray, Stephen S.; Takahashi, Tadayuki. *Proc.SPIE*, **7732**, 77324Q.